Crystal Structure and Thermochemical Properties of a First Scandium Borophosphate, $Sc(H_2O)_2[BP_2O_8]\cdot H_2O$

Bastian Ewald, Yurii Prots, Christian Kudla, Daniel Grüner, Raul Cardoso-Gil, and Rüdiger Kniep*

Max-Planck-Institut für Chemische Physik fester Stoffe, Nöthnitzer Strasse 40, 01187 Dresden, Germany

Received July 19, 2005

Crystalline samples of scandium borophosphate, $Sc(H_2O)[BP_2O_8]\cdot H_2O$, were synthesized hydrothermally from acidic suspensions of scandium sesquioxide and boric and phosphoric acid at 443 K. The chiral crystal structure (space group $P6_522$ (No. 179), $a = 957.52(3)$ pm, $c = 1581.45(6)$ pm, $Z = 6$) was solved from single-crystal data and contains helical chain anions $^1_\infty[BP_2O_8^{3-}]$ of alternating borate and phosphate tetrahedra interconnected by $ScO_4(H_2O)_2$ coordination octahedra. On thermal treatment, a reversible release of the hydrate water from the structural channels is observed, and rehydation appears as soon as the compound is exposed to air moisture for at least 1 day. X-ray powder diffractions show that the structure is retained during the de-/rehydration process. Both the crystal structure of the dehydrated phase, $Sc(H_2O)_2[BP_2O_8]$ ($a = 953.5(1)$ pm, $c = 1576.8(2)$ pm), and that of the rehydrated phase, which is identical to the hydrothermal product, were refined from X-ray powder data with Rietveld methods. When the dehydrated phase is exposed to an ammonia atmosphere, NH_3 absorption is observed.

Introduction

With all the research on borophosphates in recent years, a large number of new compounds have been reported, dense structures as well as templated solids that comprise microporous frameworks hosting template cations or molecules.[1,2] A large variety in borophosphate partial structures has been found, similar to that found in silicates and alumosilicates.[3] In all those structures, although they comprise a large range of borate to phosphate units (B:P ratio), certain ratios seem to be preferred; some anionic partial structures are found more frequently than others.

A large group of borophosphates (and metalloborophosphates) with B:P = 1:2 contains loop-branched chain anions built from tetrahedral BO_4 and PO_4 groups with a nominal composition of $[BP_2O_8^{3-}]$. These are wound around a 6-fold screw axis, forming helices that are left-handed (6_1) or right-handed (6_5). A large variety of cations and combinations of cations are known to charge balance the three negative charges per formula unit of the anion.[1,2] Even organic molecule ions can be embedded, as shown for a templated zincoborophosphate.[4] The cations occupy the voids between the borophosphate helices; because of the different sizes and charges of the cations, the helices are considerably compressed or expanded. This flexibility in the anionic partial structure seems to be one of the reasons for the large diversity of compounds crystallizing in this family of borophosphates. Focusing on the compounds with triple-charged cations, $M^{III}(H_2O)_2[BP_2O_8]\cdot H_2O$, we have found only two examples that have been reported so far, with M^{III} = Fe,[5] In.[6] The title compound, which represents the first scandium borophosphate, is a new example in this group of isostructural borophosphates.

An interesting aspect of the helical borophosphates is the presence of two chemically different types of water in the crystal structures. This can lead to interesting thermal behavior, as shown for the closely related compound $NaZn(H_2O)_2[BP_2O_8]\cdot H_2O$, which reversibly dehydrates (releasing the coordination water) to $Na[ZnBP_2O_8]\cdot H_2O$, a zincoborophosphate with CZP topology.[7] The compound $Fe(H_2O)_2[BP_2O_8]\cdot H_2O$ shows a similar two-step mass loss, releasing 2 molecules of water per formula unit in the first step.[5] In contrast to that, the title compound first releases the hydrate water (1 molecule per formula unit) upon thermal treatment up to 573 K. This step is reversible, and rehydration appears as soon as the sample is exposed to air moisture. In the de-/rehydration process, the microporous chiral network is retained, and the crystal structures of the intermediate phase $Sc(H_2O)_2[BP_2O_8]$ as well as the rehydrated phase were refined by Rietveld methods. It is the first time a reversible release of the hydrate water exclusively could be structurally proven in this family of borophosphates. The removal of water from the rigid chiral open-framework structure (in terms of connectivity) may generate phases with high levels of catalytic activities. In first experiments, the dehydrated phase absorbs small amounts of ammonia on exposure to

* To whom correspondence should be addressed. E-mail: kniep@cpfs.mpg.de.

(1) Kniep, R.; Engelhardt, H.; Hauf, C. *Chem. Mater.* **1998**, *10*, 2930.
(2) Ewald, B.; Kniep, R. In preparation.
(3) Liebau, F. *Structural Chemistry of Silicates*; Springer-Verlag: Berlin, 1985.
(4) Liu, W.; Li, M. R.; Chen, H. H.; Yang, X. X.; Zhao, J. T. *J. Chem. Soc., Dalton Trans.* **2004**, 2847.
(5) Yilmaz, A.; Bu, X. H.; Kizilyalli, M.; Stucky, G. D. *Chem. Mater.* **2000**, *12*, 3243.
(6) Ewald, B.; Prots, Yu.; Menezes, P.; Kniep, R. *Z. Kristallogr.−New Cryst. Struct.* **2004**, *219*, 351.
(7) Boy, I.; Stowasser, F.; Schäfer, G.; Kniep, R. *Chem.−Eur. J.* **2001**, *7*, 834.

10.1021/cm051577o CCC: $33.50
Published on Web 12/31/2005

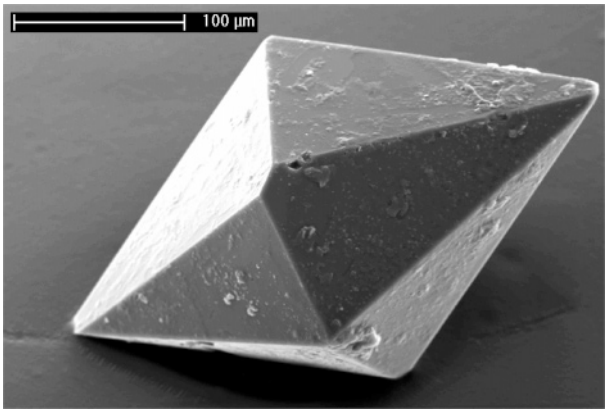

Figure 1. SEM image of a representative $Sc(H_2O)_2[BP_2O_8]\cdot H_2O$ crystal. Specimen with a distorted hexagonal bipyramidal shape were grown to a size of 0.5 mm.

a dynamic ammonia atmosphere. Preliminary results of this work have already been presented as a conference contribution.[8]

Experimental Section

Synthesis and Characterization. Single-phase samples of $Sc(H_2O)_2[BP_2O_8]\cdot H_2O$ were yielded hydrothermally in Teflon autoclaves (V = 20 mL) from acidic suspensions of scandium oxide and boric and phosphoric acid. In a molar ratio of 3:4:6 (Sc:B:P), mixtures of 0.750 g (5.44 mmol) of Sc_2O_3 (ABCR, 99.9%), 0.897 g (14.51 mmol) of H_3BO_3 (Roth, 99.9%), and 2.508 g (21.76 mmol) of H_3PO_4 (Merck, 85%) were homogenized in 10 mL of water and acidified with 1.5 mL of concentrated HCl (Merck). By evaporating the water, we concentrated the mixture to form a colorless nontransparent gel that was then treated hydrothermally at 443 K (filling degree of the autoclave: 30%). After a reaction time of 14 days, the autoclave was allowed to cool to room temperature, and the raw product was separated from the mother liquor by vacuum filtration. The transparent and colorless crystalline samples were washed with hot water, filtered, and washed again with acetone before they were dried in air at 333 K.

The elemental composition of the reaction product was investigated by means of inductively coupled plasma optical emission spectroscopy (ICP-OES) on a Varian Vista RL spectrometer with radial plasma observation. The result is the average from three measurements of a powdered sample dissolved in acids (HNO_3, HCl) after soda potash digestion. With an Sc:B:P ratio of 1.00(1):1.00(5):2.06(2), the obtained composition agrees well with the chemical formula determined by single-crystal structure refinement.

X-ray powder investigations identified the compound as a member of the group of isotypic borophosphates $M^{III}(H_2O)_2[BP_2O_8]\cdot H_2O$ (M^{III} = Fe,[5] In[6]). Single crystals of only slightly distorted hexagonal bipyramidal shape (Figure 1) were grown to a size of 0.5 mm. Specimens with regular hexagonal trapezohedral shape (also in correspondence with crystal class 622) have not been observed. Fragments of the hexagonal bipyramidal crystals, suitable for single-crystal structure determination, were selected by means of homogeneous extinction of polarized light and glued to glass fibers with two-component epoxy resin.

Decomposition Studies and Phase Analyses. Difference thermal analysis (DTA) and thermogravimetry (TG) experiments were performed in a Netzsch STA 409C/CD simultaneous analyzer utilizing Al_2O_3 crucibles and type S thermocouples. The thermal stability was investigated between room temperature and 1373 K with heating/cooling rates of 10 K/min in a dynamic argon atmosphere (gas flow 0.1 L/min). Additionally, the argon gas (Messer-Griesheim, 99.999%) was purified by being passed over zeolite molecular sieves (Roth 3 Å, BTS-catalyst, Merck). The measurements, experimentally corrected for buoyancy, reveal a total mass loss of 18.0% between 400 and 1100 K in three steps (Figure 2, top). In the simultaneously recorded DTA data, three endothermic signals were observed, at 442 K (onset 380 K), 671 K (onset 631 K), and 696 K (onset 686 K).

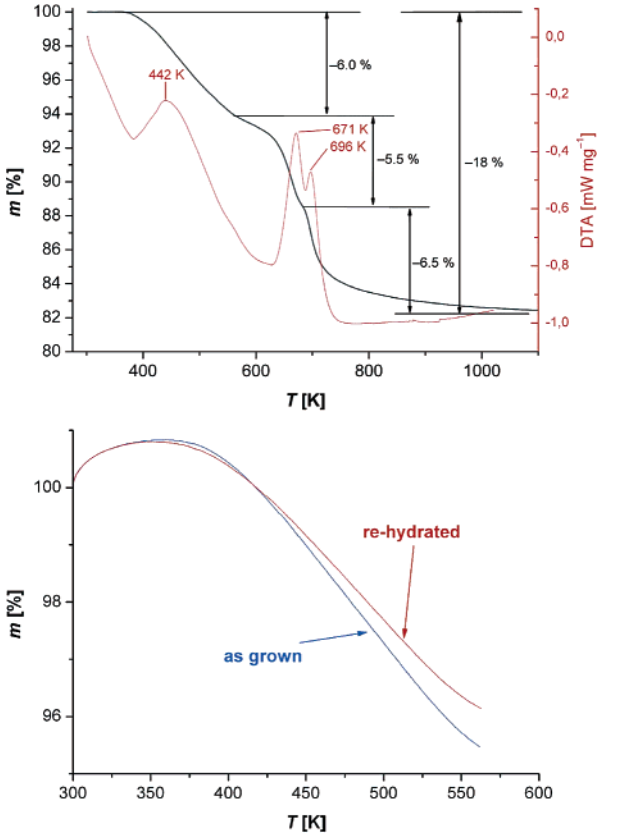

Figure 2. DTA-TG plot (top) showing a total mass loss of 18.0% between 373 and 1100 K in three steps. Three endothermic effects were recorded, at 442 K (onset 380 K), 671 K (onset 631 K), and 696 K (onset 686 K). The first step (6.0%) agrees well with the calculated loss of 1 molecule of H_2O per formula unit (hydrate water). In the second and third steps, the mass is reduced another 12.0% (5.5% + 6.5%), in agreement with the release of coordination water. As shown in a repeated TG measurement (bottom, measurements not corrected for buoyancy), the first step is reversible if a sample after dehydration (red curve) was exposed to air moisture (blue curve). After the release of 3 molecules of water per formula unit, the structure is disintegrated, as shown by powder diffraction.

In the first step, between 360 and 570 K, the weight is reduced by 6.0%, which agrees well with the release of 1 molecule of water per formula unit ($\Delta m_{calcd}/m = -6.0\%$) and with the first endothermic peak observed in the DTA measurement (T = 442 K). This process is reversible, and samples show nearly the same mass loss again when exposed to air moisture after the first dehydration step for at least 1 day (Figure 2, bottom). To characterize the dehydrated phase, we heated a sample of the hydrothermal product to 573 K; it was held at that temperature for 60 min, and was subsequently kept under inert conditions after being cooled to room temperature to avoid any rehydration. A second sample was exposed to air moisture for days after the thermal treatment in order to obtain a fully rehydrated phase for characterization. X-ray powder investigations of both the dehydrated and rehydrated phases indicated that the structural arrangement was retained during the de-/rehydration; the diffraction patterns were indexed with a hexagonal lattice. Both

(8) Ewald, B.; Prots, Yu.; Kniep, R. *Z. Anorg. Allg. Chem.* **2004**, *630*, 1720.

structures could be refined by Rietveld methods as described in the following.

In the second and third steps of mass loss, between 570 and 1100 K, the weight decreases by another 12.0% (5.5% + 6.5%), which matches the loss of 2 molecules of water per formula unit ($\Delta m_{calcd}/m = -12.0\%$). After releasing an equivalent of 3 molecules of water in total, the structure irreversibly decomposes to BPO_4 and another, still unidentified phase, as evidenced by X-ray powder investigations. The three-step behavior in the TG and DTA measurements indicates that the coordination water is released in two steps.

Crystal Structure Determinations. *Hydrothermal Product—Single-Crystal Structure Analysis*. An individual crystal of $Sc(H_2O)_2[BP_2O_8]\cdot H_2O$ (irregular fragment, 0.125 mm × 0.090 mm × 0.075 mm) suitable for data collection was mounted on a Rigaku AFC7 diffractometer equipped with a Mercury CCD detector. Two measurements with long and short exposure times were performed to obtain accurate intensities of strong and weak reflections. The data sets were combined and scaled using the program XPREP.[9] The resulting data set ($-14 \le h \le 14$, $-14 \le k \le 14$, $-24 \le l \le 17$; $5.54° \le 2\theta \le 66.98°$) was corrected for absorption using the multiscan procedure.

The analysis of the reflections indicated Laue symmetry 6/*mmm* with systematic absences of reflections 000*l* for all $l = 2n + 1$. From the two possible space groups, $P6_122$ and $P6_522$, the latter was chosen for the investigated individual crystal, and the refinement resulted in a Flack parameter $x = -0.04(5)$.

By interpreting Patterson maxima,[10] we obtained initial atomic positions of Sc, P, and some of the oxygen atoms. In the structure refinement by the least-squares methods,[10] the remaining atom sites were assigned according to maxima in the difference Fourier maps that were observed between the refinement steps. Initially, the hydrate water (O6) was located on the special position 6*a* with the coordinates 0.170, *x*, 5/6, but the refinement resulted in a large thermal parameter and the appearance of additional maxima in the difference Fourier maps at a distance of 63 pm from the O6 atoms. Thus, a split model was assumed in which O6 is located on the general position 12*c* close to the 6*a* site with an occupancy factor of 0.5 (in accordance with 1 molecule of H_2O per formula unit).

All non-hydrogen atoms were refined with anisotropic displacement parameters. From the difference Fourier maps, only the hydrogen atoms close to O5 (coordination water) were located on the general position 12*c*. Whereas the isotropic displacement parameters of the protons had to be restrained ($1.2 \times U_{iso}$(O)), the positions were refined as free variables during the final refinement steps (0.414(6), 0.269(5), and 0.797(3) for H51, and 0.561(5), 0.376(5), and 0.792(2) for H52). For the calculation of interatomic distances and angles, we refined unit cell parameters of the hexagonal lattice from X-ray powder data calibrated with LaB_6 as an internal standard.

A summary of the crystallographic data and refinement parameters is given in Table 1, and the refined atomic coordinates are listed in Table 2, along with those of the dehydrated and rehydrated phases.

Rietveld Refinements of the Dehydrated and Rehydrated Phase. X-ray powder patterns for Rietveld refinements of the dehydrated phase $Sc(H_2O)_2[BP_2O_8]$ and of the rehydrated product $Sc(H_2O)_2[BP_2O_8]\cdot H_2O$ were recorded on a STOE Stadi MP diffractometer equipped with a primary-beam germanium monochromator using Cu $K\alpha_1$ radiation. The powder samples (~50 μm particle size) were loaded into glass capillaries with a 0.3 mm inner diameter. Continuous scan data were collected within a range of $5° \le 2\theta \le 110°$. The collected powder diffraction data of both the dehydrated and rehydrated phases show similar patterns, but except for a shift in reflection positions (the unit cell of the dehydrated phase is slightly smaller), small differences are observed for the intensities.

Rietveld refinements were carried out using the Jana2000 program package.[11] During the initial LeBail decomposition, we obtained starting parameters for the profiles, cell parameters, and background. The background was described by a Legendre polynomial (18 terms), whereas Pseudo-Voigt functions were fitted to the peak profiles. To describe the asymmetry of the peaks, we used a function proposed by Berar and Baldinozzi with four parameters.[12] Cell parameters were refined, leading to values similar to those obtained from calibrated powder diffraction experiments.

As a starting model for the Rietveld refinements, the single-crystal data for the hydrothermal product without the hydrogen atoms were used for the rehydrated phase. In the case of the dehydrated phase, the hydrate water (O6) was removed from the starting model. The isotropic displacement parameters of all oxygen atoms were restrained to keep them equal during the first cycles.

Table 1. Crystallographic Data and Refinement Parameters for Hydrothermally Grown $Sc(H_2O)_2[BP_2O_8]\cdot H_2O$[a]

formula	$Sc(H_2O)_2[BP_2O_8]\cdot H_2O$
fw (g mol^{-1})	299.76
space group	$P6_522$ (no. 179)
formula units	$Z = 6$
a (pm)	957.52(3)
c (pm)	1581.45(6)
V (nm^3)	1.25569(7)
calcd density (Mg m^{-3})	2.378
wavelength, λ (pm)	Mo Kα, 71.073
abs coeff, μ Mo Kα (mm^{-1})	1.313
no. of reflns collected	13913
no. of independent reflns	1585 [R(int) = 0.027]
refined params	82
GOF on F^2	1.275
final R indices ($I > 2\sigma(I)$)	R1 = 0.033
	wR2 = 0.078
R indices (all data)	R1 = 0.034
	wR2 = 0.080
flack param *x*	−0.04(5)
largest diff. peaks (10^6 e pm^{-3})	−0.515/0.473

[a] The residuals are defined as follows: $R_{int} = \sum(F_o^2 - F_o^2(\text{mean}))/\sum(F_o^2)$; $R1 = \sum(|F_o| - |F_c|)/\sum|F_o|$; $wR2 = \{\sum[w(F_o^2 - F_c^2)]^2/\sum[w(F_o^2)^2]\}^{1/2}$.

Table 2. Rietveld Analysis of the X-ray Powder Diffractograms of the Dehydrated and Rehydrated Phase: Crystallographic Data and Refinement Parameters

	dehydrated	rehydrated
formula[a]	$Sc(H_2O)_2[BP_2O_8]$	$Sc(H_2O)_2[BP_2O_8]\cdot H_2O$
cryst syst	hexagonal	hexagonal
space group	$P6_522$ (No. 179)	$P6_522$ (No. 179)
a (pm)	953.5(1)	957.4(1)
c (pm)	1576.8(2)	1580.7(1)
Z	6	6
N/*P*[b]	5250/66	5250/70
R_{wp}[c] (%)	4.31	4.68
R_B[d] ($I > 3\sigma(I)$) (%)	3.66	3.44
R_B[d] (all data)	3.77	3.48
GOF[e]	1.33	2.89

[a] Hydrogen atoms have not been included in the refinement. [b] No. of y_i/no. of variables. [c] $R_{wp} = (\sum w_i(y_{oi} - y_{ci})^2/(\sum w_i(y_{oi}^2))^{1/2}$. [d] $R_B = \sum|I_{ko'} - I_{kc}|/\sum I_{o'}$ with I_k intensity assigned to *k*th Bragg reflection. [e] GOF = $(\sum w_i(y_{oi} - y_{ci})^2/(N - P))^{1/2}$.

(9) *XPREP: Data Preparation & Reciprocal Space Exploration*; Bruker AXS: Karlsruhe, Germany, 2004.
(10) *SHELXS-97/2: Program for the Solution of Crystal Structures and SHELXL-97/2: Program for Crystal Structure Refinement*; Universität Göttingen: Göttingen, Germany, 1997.
(11) Petříček, V.; Dušek, M.; Palatinus, L. *Jana2000. The Crystallographic Computing System*; Institute of Physics: Praha, Czech Republic, 2000.
(12) Berar, J.-F.; Baldinozzi, G. *J. Appl. Crystallogr.* **1993**, *26*, 128.

Table 3. Atomic Coordinates (protons excluded) and Thermal Parameters U_{iso} (10 pm^2) of the Refined Structures of the Hydrothermal Product (I), the Dehydrated Phase (II), and the Rehydrated Phase (III)

atom	site	compd	*x*	*y*	*z*	U_{iso}
Sc	6*b*	I	0.5552(1)	0.1105(1)	0.75	12(1)
		II	0.5542(4)	0.1085(7)	0.75	23(3)
		III	0.5556(3)	0.1111(7)	0.75	18(3)
B	6*b*	I	0.2919(3)	0.1460(2)	0.4167	13(1)
		II	0.292(4)	0.146(2)	0.4167	17(10)
		III	0.289(4)	0.145(2)	0.4167	30(11)
P	12*c*	I	0.3765(1)	0.1687(1)	0.5842(1)	11(1)
		II	0.3789(6)	0.1667(7)	0.5851(3)	17(3)
		III	0.3774(6)	0.1682(7)	0.5845(4)	16(3)
O1	12*c*	I	0.4042(2)	0.1711(2)	0.4867(1)	14(1)
		II	0.410(1)	0.173(1)	0.4894(7)	21(4)
		III	0.408(1)	0.173(2)	0.4887(7)	15(4)
O2	12*c*	I	0.2063(2)	0.242(2)	0.6029(1)	14(1)
		II	0.212(2)	0.027(1)	0.6031(8)	18(4)
		III	0.207(2)	0.028(1)	0.6030(8)	17(4)
O3	12*c*	I	0.5037(2)	0.1436(2)	0.6264(1)	18(1)
		II	0.509(1)	0.145(1)	0.6262(8)	17(4)
		III	0.506(2)	0.146(1)	0.6240(8)	13(4)
O4	12*c*	I	0.3777(2)	0.3206(2)	0.6112(1)	19(1)
		II	0.387(1)	0.322(2)	0.6165(7)	20(4)
		III	0.375(2)	0.319(2)	0.6135(8)	22(5)
O5	12*c*	I	0.4949(3)	0.2919(3)	0.7837(2)	33(1)
		II	0.490(1)	0.297(1)	0.7840(7)	28(4)
		III	0.489(1)	0.291(1)	0.7872(8)	35(5)
O6	12*c*	I	0.180(1)	0.159(1)	0.853(1)	91(5)
		II				
		III	0.187(3)	0.166(3)	0.855(2)	38(10)

After the initial relaxation, the thermal displacement parameters were refined isotropically without restraints. Both data sets were tested for a possible occupancy of the O6 position. Whereas for the rehydrated phase a full occupancy was found, no electron density was found for this position in the difference Fourier maps for the dehydrated phase. In the final cycles of the refinement, the thermal displacement parameters of Sc and P were refined in an anisotropic approximation. A summary of the crystallographic data as well as the refinement parameters for both phases is given in Table 2. The refined atomic positions are listed in Table 3 in direct comparison to those of the hydrothermal product. Intensity vs 2θ plots of the observed and calculated powder patterns of both refinements are shown in Figure 3 (top: dehydrated, bottom: rehydrated). As no significant structural differences between the hydrothermal product and the rehydrated phase have been found, the structures were treated as though they are identical.

Ammonia Absorption. To investigate the absorption activity of the dehydrated phase when exposed to an ammonia atmosphere, we performed the dehydration step in a tube furnace equipped with a quartz reaction tube with gas inlets for dynamic flow atmospheres. The ground hydrothermal product was placed in an Al_2O_3 crucible in the reaction tube; it was heated to $T = 563$ K (10 K min^{-1}), kept at T for 60 min, and cooled to room temperature (10 K min^{-1}) in a dynamic argon atmosphere. The atmosphere was then changed to an ammonia flow, and the sample was exposed for 6 h. The obtained powder shows only small differences in the hexagonal lattice parameters ($a = 955(1)$ pm, $c = 1579(1)$ pm)[13] when compared to those of the hydrothermal product.

Infrared Spectroscopy. The infrared spectra of all phases were recorded using a Fourier transform spectrometer (Bruker, IFS 66) equipped with a glowbar and a DTGS detector. Typically, the samples contained 150 mg of KBr and 1.0−2.0 mg of sample. Absorption spectra were collected in the range 4000−500 cm^{-1}, and were analyzed with respect to the characteristic bands indicating the presence or absence of hydrate water and ammonia. Representative spectra are shown in Figure 4.

(13) *Stoe Win XPOW*; Stoe & Cie GmbH: Darmstadt, Germany, 1999.

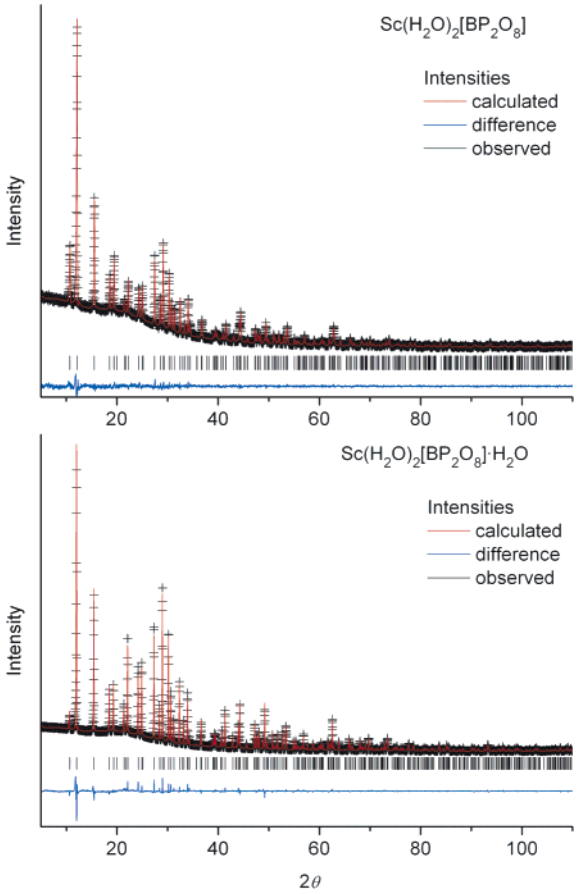

Figure 3. Rietveld refinements of the dehydrated ($Sc(H_2O)_2[BP_2O_8]$, top) and rehydrated ($Sc(H_2O)_2[BP_2O_8]\cdot H_2O$, bottom) phases: observed and calculated powder patterns, Bragg reflection markers, and difference curves ($I_{obs} - I_{calcd}$).

Results and Discussion

Crystal Structure Description. The crystal structures of $Sc(H_2O)_2[BP_2O_8]\cdot H_2O$ (hydrothermal product and rehydrated phase) and $Sc(H_2O)_2[BP_2O_8]$ (dehydrated phase) contain one-dimensional infinite loop-branched borophosphate helices $^1_\infty[BP_2O_8^{3-}]$ built of distorted borate and phosphate tetrahedra that are arranged in an alternating fashion. Whereas the borate groups share all oxygen vertexes with adjacent phosphate tetrahedra, the PO_4 units are connected only to two BO_4 units. The resulting structural motif can be described as a 1D infinite arrangement of four-membered rings of tetrahedra connected via common borate groups. The borophosphate strands, wound around a 6_5 screw axis, are arranged parallel [001] (Figure 5). Each helix is, because of symmetry, surrounded by six adjacent chains at equal distance; thus, the arrangement can be illustrated as a dense packing of rods (Figure 6). Scandium is 6-fold coordinated by four oxygen atoms that originate from phosphate groups and two water molecules. The resulting distorted $ScO_4(H_2O)_2$ coordination octahedra intra- and interconnect the helical strands (Figure 5). Whereas in the crystal structure of $Sc(H_2O)_2[BP_2O_8]\cdot H_2O$, hydrate water (O6) is located inside the helical channels (as shown in Figures 5 and 6), these

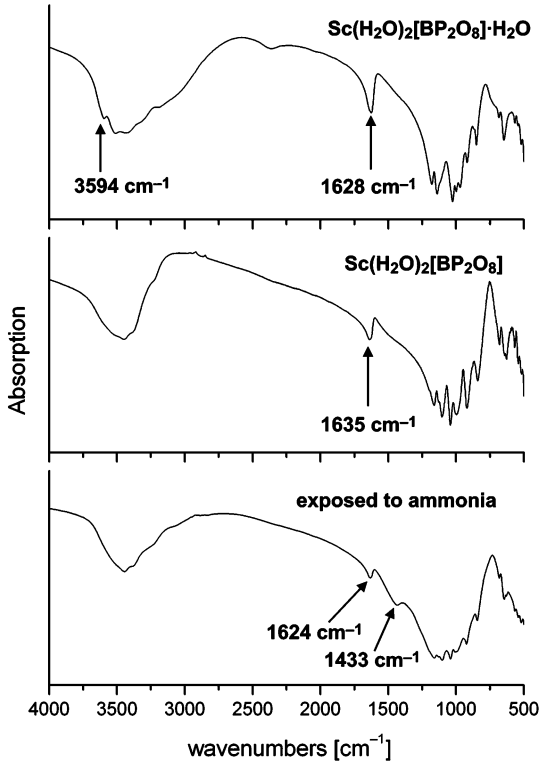

Figure 4. FTIR spectrum of $Sc(H_2O)_2[BP_2O_8]\cdot H_2O$ (top) in comparison with those of the dehydrated $Sc(H_2O)_2[BP_2O_8]$ (middle) and the sample exposed to an ammonia atmosphere after the first dehydration step (bottom). All phases show the presence of water by characteristic absorptions at about 1630 cm^{-1} (H_2O deformation) and between 3000 and 3600 cm^{-1} (O−H stretching). In accordance with the loss of water, the dehydrated phase shows fewer features of O−H stretching, and the absorption at about 1630 cm^{-1} is significantly weakened. For the sample exposed to an ammonia atmosphere, a new absorption at 1433 cm^{-1} appears, which is attributed to ammonia.

positions are unoccupied in the dehydrated phase $Sc(H_2O)_2[BP_2O_8]$.

On dehydration, the unit cell shrinks by 1.1% with a constant aspect ratio *a*/*c* of 0.605, and only small differences in the interatomic arrangement are observed. Within the range of the estimated errors, the bond distances of the dehydrated phase (B−O = 147(2) and 153(2) pm, P−O = 150(1)−153(1) pm, and Sc−O = 206(1)−223(2) pm), the hydrothermal product (B−O = 146.2(2) and 147.8(1) pm, P−O = 151.0(2)−156.2(1) pm, and Sc−O = 205.2(2)−215.4(2) pm), and the rehydrated phase (B−O = 148(4) and 153(3) pm, P−O = 149(2)−154(1) pm, and Sc−O = 208(2)−220(1) pm) show only small deviations. Factoring in the standard deviations, we found only small differences for the bond angles between adjacent oxygen atoms in the distorted coordination polyhedra if the arrangement in the dehydrated $Sc(H_2O)_2[BP_2O_8]$ (O−B−O = 102(2)−113(2)°, O−P−O = 105.9(9)−112.0(8)°, and O−Sc−O = 82.5(6)−98.3(5)°) is compared with those of the hydrated (O−B−O = 101.8(2)−113.53(8)°, O−P−O = 107.03(8)−114.5(8)°, and O−Sc−O = 83.43(7)−96.22(6)°) and rehydrated (O−B−O = 102(2)−114(1)°, O−P−O = 105(1)−114.5(8)°, and O−Sc−O = 82.5(7)−95.3(7)°) phases. It is conspicuous that the polyhedra in the crystal structures refined by Rietveld methods differ from those of the single-crystal structure. For example, the B−O distances are systematically larger and the P−O distances smaller than those in the single-crystal

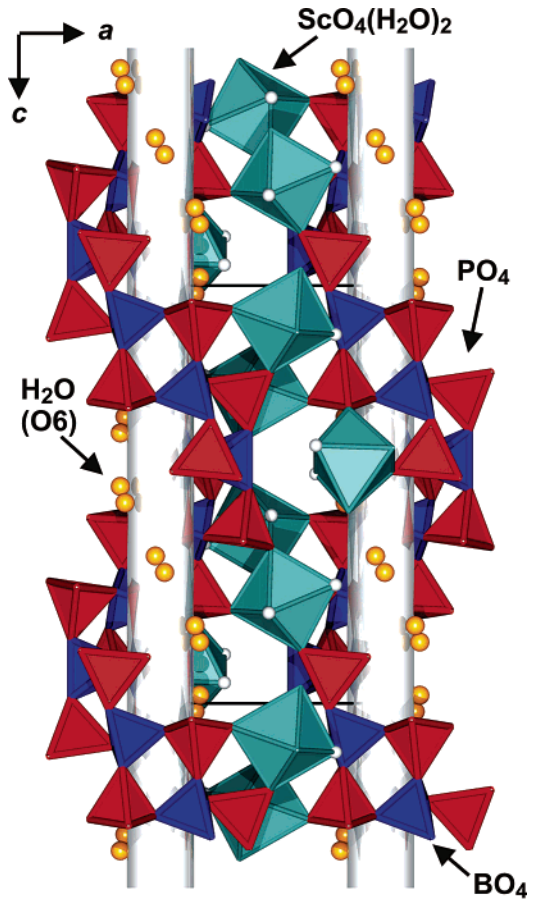

Figure 5. Crystal structure of $Sc(H_2O)_2[BP_2O_8]\cdot H_2O$. Helical chains $^1_\infty[BP_2O_8^{3-}]$, running along [001], are placed on the edges of the hexagonal unit cell, and are interconnected via $ScO_4(H_2O)_2$ coordination octahedra. The hydrate water (split position O6) is located in the helical channels. These positions are unoccupied in the crystal structure $Sc(H_2O)_2[BP_2O_8]$.

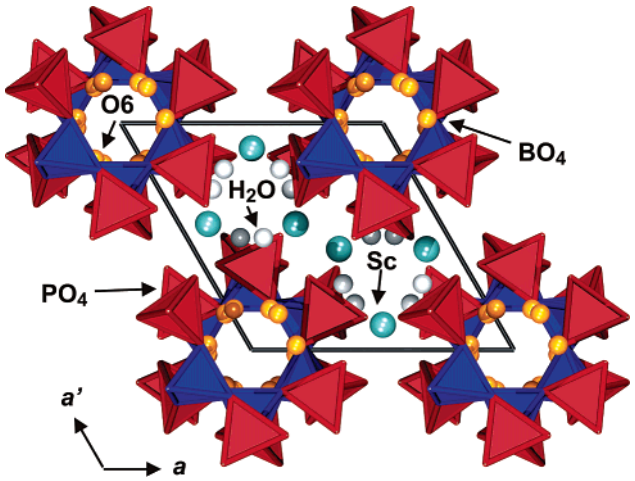

Figure 6. View along [001] of the helical borophosphates, illustrating the arrangement of the chains in a dense rod-packing motif and the location of the hydrate water (O6) inside the channels. This position is occupied only in hydrated $Sc(H_2O)_2[BP_2O_8]\cdot H_2O$.

structure solution. This observation can be made in other structure refinements of borophosphates as well.[7]

Structural Classification. With a ratio of borate to phosphate units (B:P) of 1:2, the helical borophosphates belong to the largest group of borophosphates comprising anionic entities with dimensionalities ranging from oligomers to layers (e.g., in $Na_2[BP_2O_7(OH)]$).[14] The only 3D network with B:P = 1:2 is present in the crystal structure M^I-

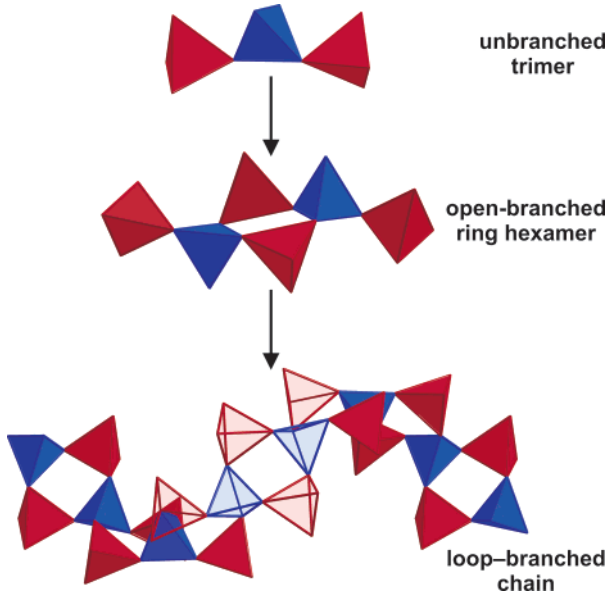

Figure 7. Hierarchical assembly of the helical chains from fundamental building units with B:P = 1:2 (phosphate tetrahedra, red; borate tetrahedra, blue). Both of the tetrahedral fragments, the unbranched trimeric unit 3□:□□□ (top) and the open-branched ring hexamer 6□:□<4□>□ (middle), exist isolated as oligomeric anions in borophosphates (see the text).

$[BeBP_2O_8]\cdot xH_2O$ ($M^I = Na^+$, K^+, NH_4^+),[15] which contains additional tetrahedral building units (BeO_4) and is therefore classified by definition as a berylloborophosphate.[1,2]

Because of their flexibility, the helical chains can host different cations and, thus, the number of known phases with this kind of anion (borophosphates and metalloborophosphates) is comparatively large. Focusing on the isotypic compounds $M^{III}(H_2O)_2[BP_2O_8]\cdot H_2O$, we found that the lattice parameters increase from $a = 945.8$ pm and $c = 1570.1$ pm for $M^{III} = Fe$[5] via $a = 957.5$ pm and $c = 1581.5$ pm for the scandium compound reported here to $a = 957.0$ pm and $c = 1587.0$ pm for the indium compound.[6] This fits well with the ionic radii of the cations in 6-fold coordination increasing in the sequence $r(Fe^{3+}$, high-spin) = 79 pm > $r(Sc^{3+}) = 89$ pm > $r(In^{3+}) = 94$ pm.[16,17]

In terms of silicate structural chemistry, the helical partial structure $^1_\infty[BP_2O_8^{3-}]$ has to be denoted as a loop-branched zwölfer single chain with 12 ("zwölf") tetrahedra in the periodic sequence of the unbranched backbone (Figure 7, bottom).[3] Disassembling the anionic partial structure to its fundamental building unit (FBU) as is proposed for borate minerals,[18,19] we found an open-branched ring hexamer (Figure 7, middle), which can be cut into simple unbranched borophosphate trimers with B:P = 1:2 (Figure 7, top). A structural descriptor to illustrate the FBU[18,19] can be written as 6□:□<4□>□ containing the information about the number of participating tetrahedra (6□) and the structural sequence (here: four-membered ring of tetrahedra <4□> with open branches □). The corresponding sequence for the trimeric unit has to be written as 3□:□□□. Both tetrahedral fragments, 6□:□<4□>□ and 3□:□□□, are found as isolated oligomeric anions in borophosphates. The ring hexamer is, for example, found in a group of isotypic compounds with the composition $M^IM^{III}[BP_2O_8(OH)]$ ($M^I = NH_4^+$, K^+, Rb^+; $M^{III} = Fe^{3+}$, In^{3+}),[20−23] and the trimeric tetrahedral anion is present in borophosphates of the type $M^IM^{III}[BP_2O_7(OH)_3]$ ($M^I = NH_4^+$, Na^+, K^+, Rb^+; $M^{III} = Al^{3+}$, V^{3+}, Fe^{3+}, Ga^{3+}, In^{3+}).[20,24−28] Sorting the anionic entities hierarchically according to their FBUs helps us to understand the formation of structural motifs such as the four-membered rings present in the anionic entity presented here.

Thermal Stability, Ammonia Absorption, and IR Spectroscopy. Two chemically different types of water molecules are present in the crystal structure of $Sc(H_2O)_2[BP_2O_8]\cdot H_2O$, hydrate water and coordination water. Whereas the latter species is part of the scandium coordination octahedra, the hydrate water (O6) is comparatively loosely held in the channels of the structure, as shown by the big thermal displacement parameters in the refined crystal structure. Thus, it is not surprising that on thermal treatment the hydrate water is released first (weight loss 6.0%). This behavior is in contrast to phases of the composition $M^IM^{II}(H_2O)_2[BP_2O_8]\cdot H_2O$ or the compound $Fe(H_2O)_2[BP_2O_8]\cdot H_2O$, which release at least one molecule of coordination water in the first dehydration step.[5,7,29] In the family of borophosphates with helical $^1_\infty[BP_2O_8^{3-}]$ anions, the reversible dehydration of $Sc(H_2O)_2[BP_2O_8]\cdot H_2O$ is the first example with structural proof that the hydrate water is exclusively released from the microporous framework. Although for Zn^{2+} the preferred coordination is four, Sc^{3+} prefers an octahedral coordination; in contrast to the coordination water in $NaZn(H_2O)_2[BP_2O_8]\cdot H_2O$, that in the Sc^{3+} compound is strongly bound. According to preliminary results for $In(H_2O)_2[BP_2O_8]\cdot H_2O$, a three-step mass loss is observed on thermal treatment. As for the title compound, only an equivalent of 1 H_2O per formula unit is released in the first step.

Small changes in the structural arrangement of the hydrated and dehydrated phases, which are mainly due to the shrinking of the unit cell by 1.1% on dehydration, prove the rigid connectivity of the flexible polyhedral framework. On release

(14) Kniep, R.; Engelhardt, H. *Z. Anorg. Allg. Chem.* **1998**, *624*, 1291.
(15) Zhang, H.; Chen, C.; Weng, L.; Zhou, Y.; Zhao, D. *Microporous Mesoporous Mater.* **2003**, *57*, 309.
(16) Shannon, R. D.; Prewitt, C. T. *Acta Crystallogr., Sect. B* **1969**, *25*, 925.
(17) Shannon, R. D.; Prewitt, C. T. *Acta Crystallogr., Sect. A* **1976**, *32*, 751.
(18) Grice, J. D.; Burns, P. C.; Hawthorne, F. C. *Can. Mineral.* **1999**, *37*, 731.
(19) Burns, P. C.; Grice, J. D.; Hawthorne, F. C. *Can. Mineral.* **1995**, *33*, 1131.
(20) Boy, I.; Cordier, G.; Eisenmann, B.; Kniep, R. *Z. Naturforsch.* **1998**, *B53*, 165.
(21) Mao, S.-Y.; Li, M.-R.; Huang, Y.-X.; Mi, J.-X.; Zhao, J.-T.; Kniep, R. *Z. Kristallogr.−New Cryst. Struct.* **2002**, *217*, 3.
(22) Huang, Y.-X.; Zhao, J.-T.; Mi, J.-X.; Borrmann, H.; Kniep, R. *Z. Kristallogr.−New Cryst. Struct.* **2002**, *217*, 163.
(23) Mi, J.-X.; Li, M.-R.; Mao, S.-Y.; Huang, Y.-X.; Wei, Z.-B.; Zhao, J.-T.; Kniep, R. *Z. Kristallogr.−New Cryst. Struct.* **2002**, *217*, 5.
(24) Huang, Y.-X.; Mi, J.-X.; Mao, S.-Y.; Wei, Z.-B.; Zhao, J.-T.; Kniep, R. *Z. Kristallogr.−New Cryst. Struct.* **2002**, *217*, 7.
(25) Huang, Y.-X.; Mao, S.-Y.; Mi, J.-X.; Wei, Z.-B.; Zhao, J.-T.; Kniep, R. *Z. Kristallogr.−New Cryst. Struct.* **2001**, *216*, 15.
(26) Mi, J.-X.; Huang, Y.-X.; Mao, S.-Y.; Zhao, J.-T.; Kniep, R. *Z. Kristallogr.−New Cryst. Struct.* **2002**, *217*, 167.
(27) Zhang, L.-R.; Zhang, H.; Borrmann, H.; Kniep, R. *Z. Kristallogr.−New Cryst. Struct.* **2002**, *217*, 477.
(28) Koch, D.; Kniep, R. *Z. Kristallogr.−New Cryst. Struct.* **1999**, *214*, 441.
(29) Kniep, R.; Will, H. G.; Boy, I.; Röhr, C. *Angew. Chem.* **1997**, *109*, 1052; *Angew. Chem., Int. Ed.* **1997**, *36*, 1013.

of the two water molecules coordinating Sc, the structure collapses.

In accordance with the structural refinements and TG curves, the infrared spectra of $Sc(H_2O)_2[BP_2O_8]\cdot H_2O$ and $Sc(H_2O)_2[BP_2O_8]$ show significant differences. The removal of the hydrate water agrees well with the weakening of the feature at about 1630 cm^{-1} (H_2O deformation)[30,31] and the less-pronounced broad absorption between 3000 and 3600 cm^{-1} (O−H stretching),[30,31] as observed for the dehydrated phase. The band at 3594 cm^{-1} disappears along with the broad shoulder close to 3000 cm^{-1} (Figure 4). If the dehydrated sample is exposed to ammonia, a new feature at 1433 cm^{-1} appears, which has to be attributed to ammonia.[31] The composition of a sample kept in air at ambient conditions (exposed to air moisture) was determined by chemical analysis. With a total amount of 0.45(3) wt % N in the sample, only an equivalent of 8.4(2)% of the hydrate water is exchanged. The powder diffractograms recorded after the experiments show that the microporous structure is retained ($a = 955(1)$ pm, $c = 1579(1)$ pm). Thus, different reaction conditions (lower temperature and vacuum during the dehydration step) and sample treatments after the reaction (keeping it in an Ar or NH_3 atmosphere) are currently under investigation in order to obtain a fully substituted product. Additionally, further experiments with a H_2S atmosphere are planned.

Conclusion

The number of borophosphates has grown steadily since the intensive research began just 10 years ago. The crystal structures comprise a large diversity in composition B:P and dimensionality of the anionic arrangements. Nevertheless, certain B:P ratios and, thus, certain structural motifs are found more frequently than others. The first scandium borophosphate, $Sc(H_2O)_2[BP_2O_8]\cdot H_2O$, is isotypic with the known compounds $M^{III}(H_2O)_2[BP_2O_8]\cdot H_2O$ (M^{III} = Fe,[5] In[6]), and belongs to a large family of borophosphates with loop-branched helical chains $^1_\infty[BP_2O_8^{3-}]$. A B:P ratio of 1:2, as in the loop-branched chain anion, is commonly found in borophosphates. To understand the formation and appearance of certain structural patterns of the same B:P ratio, we found a structural hierarchy in which the anionic partial structures are disassembled into simple oligomeric fundamental building units to be helpful. Starting from a simple unbranched trimeric unit of tetrahedra (3□:□□□), we can illustrate the formation of the open-branched ring chain arrangement via a loop-branched hexamer (6□:□<4□>□) in simple condensation steps.

The reversible dehydration to $Sc(H_2O)_2[BP_2O_8]$, in which the polyhedral arrangement is retained, as proven by the structural refinements of the de- and rehydrated phases, shows the stability of the microporous framework. Similar dehydration behavior has been observed for other compounds in this family of borophosphates as well, but the sequence in which hydrate water and coordination water are released is influenced by the cations present in the structure.

The stability of the microporous framework may indicate the applicability of these compounds as interesting functional materials. These first experiments on ammonia absorption of dehydrated $Sc(H_2O)_2[BP_2O_8]$ exposed to a NH_3 atmosphere show a certain activity, but the low absorption makes further experiments with different reaction conditions necessary. Additionally, absorption experiments with different helical borophosphates and with different molecules may lead to interesting results.

Acknowledgment. We are grateful to Dr. Rainer Niewa and Susann Müller for DTA/TG measurements. We thank Dr. Gudrun Auffermann, Anja Völzke, and Ulrike Schmidt for chemical analyses. Additionally, we thank Steffen Hückmann for numerous powder diffraction measurements and Prashanth Menezes for SEM images.

Supporting Information Available: Crystallographic data of the hydrothermal product $Sc(H_2O)_2[BP_2O_8]\cdot H_2O$, the dehydrated phase $Sc(H_2O)_2[BP_2O_8]$, and the rehydrated $Sc(H_2O)_2[BP_2O_8]\cdot H_2O$ in CIF format. This material is available free of charge via the Internet at http://pubs.acs.org. The crystallographic data may also be obtained from the Fachinformationzentrum Karlsruhe, D-76344 Eggenstein-Leopoldshafen (fax: 49-7247-808-666; E-mail: crysdata@fiz-karlsruhe.de) by quoting the name of the author, the citation of the paper, and the depository numbers CSD-416075 for $Sc(H_2O)_2[BP_2O_8]\cdot H_2O$ (hydrothermal product) and CSD-416074 for $Sc(H_2O)_2[BP_2O_8]$ (dehydrated phase).

CM051577O

(30) Corbridge, D. E. C.; Lowe, E. J. *J. Chem. Soc. (London)* **1954**, 493.
(31) Nakamoto, K. *Infrared and Raman Spectra of Inorganic and Coordination Compounds, Part A: Theory and Applications in Inorganic Chemistry*; Wiley-Interscience: New York, 1997.